Original Paper

Cellular Physiology and Biochemistry

Cell Physiol Biochem 2007;20:241-254

Accepted: March 15, 2007

Infections with Human Rhinovirus Induce the Formation of Distinct Functional Membrane Domains

Stephan Dreschers, Peter Franz[1], Claudia Alexandra Dumitru, Barbara Wilker, Klaus Jahnke[1] and Erich Gulbins

Department of Molecular Biology and [1]Department of Otorhinolaryngology, University of Duisburg-Essen

Key Words

Rhinovirus • Membrane rafts • Ceramide • Gangliosides • Acid sphingomyelinase

Abstract

The plasma membrane contains distinct domains that are characterized by a high concentration of sphingolipids and cholesterol. These membrane microdomains also referred to as rafts, seem to be intimately involved in transmembranous signaling and often initiate interactions of pathogens and the host cell membranes. Here, we investigated the further reorganization of membrane rafts in cultured epithelial cells and *ex vivo* isolated nasal cells after infection with rhinoviruses. We demonstrate the formation of ceramide-enriched membrane platforms and large glycosphingolipid-enriched membrane domains and the co-localization of fluorochrome-labeled rhinoviruses with these membrane domains during attachment and uptake of human rhinovirus. Destruction of glycosphingolipid-enriched membrane domains blocked infection of human cells with rhinovirus. Furthermore, our studies indicate that the activation of the acid sphingomyelinase (ASM) is intrigued in the formation of ceramide- or GM1-enriched membrane platforms. Inhibition of the ASM reduces the number of ceramide-enriched platforms and glycosphingolipid-enriched membrane domains. These data reveal a critical role of the ASM for the formation of membrane platforms and infection of human cells with rhinoviruses.

Introduction

The classical fluid mosaic model of the cell membrane suggests a random distribution of lipids and proteins in the cell membrane [1]. However, this view was challenged by many recent studies indicating that sphingolipids and cholesterol spontaneously separate from glycophospholipids in the cell membrane to form distinct microdomains [2, 3]. Sphingolipids bind to each other via hydrophilic interactions between their headgroups and the saturated fatty acid side chains, respectively. Void spaces between the bulky glycosphingolipids appear to be filled with cholesterol. The sterol ring system interacts thightly with the sphingosine moiety of the sphingolipids via hydrogen boundings between the C3 hydroxylgroup and the hydrophilic headgroup of sphingomyelin. These interactions result in a lateral stabilization and facilitate

KARGER

Fax +41 61 306 12 34
E-Mail karger@karger.ch
www.karger.com

1015-8987/07/0204-0241$23.50/0

Accessible online at:
www.karger.com/cpb

Dr. Stephan Dreschers
Dept. of Molecular Biology, University of Duisburg-Essen
Hufelandstrasse 55, 45122 Essen (Germany)
Tel. +49-201-723-3418, Fax +49-2001-723-5974
E-Mail stephan.dreschers@uni-essen.de

the formation of distinct membrane domains termed rafts [3, 4].

Recent studies indicate that rafts are also central for the infection of mammalian cells with pathogens including bacteria, such as *Pseudomonas aeruginosa*, *Salmonella typhi*, *Shigella enterocolitica*, *Vibrio cholerae*, *Clostridium difficile*, and viruses, e.g. Influenza virus, HIV-1 (human immunodeficiency virus type 1), Respiratory syncytial cell virus, SV40 (simian virus type 40) or measles virus [5-17, for review see 18]. However, the detailed role of rafts for cellular infection with pathogens requires definition.

In the present study we investigated the role of membrane rafts for the infection of mammalian respiratory epithelial cells with human rhinoviruses.

Rhinoviruses belong to the picornaviridae family and are small, positive-stranded RNA viruses. Infection is restricted to the upper airway epithelium resulting in the common cold. Rhinoviruses are classified into two subgroups, designated the minor and the major group. The attachment and entry of minor group rhinoviruses is mediated via the LDL (low density lipoprotein) receptor family [19-21], whereas the major group rhinoviruses bind to the ICAM-1 (intercellular adhesion molecule type 1, CD54) receptor [22]. However, the details of rhinovirus invasion remain to be clarified, particularly since ICAM-1 expression has not been detected in nasal epithelial cells [23, 24]. Upon binding of the virus to its receptor, rhinoviruses are rapidly internalized into vesicles, the genomic RNA is finally released into the cytoplasm and is directly translated into a single polypeptide chain, which is cleaved into four capsid proteins and the viral polymerase. Recent data indicated that induction of specialized membrane domains, i.e. ceramide-enriched membrane platforms, play a crucial role for infection of mammalian cells with rhinovirus [25]. The formation of ceramide-enriched membrane platforms requires the activation of the acid sphingomyelinase (ASM). Fibroblasts isolated from Niemann-Pick patients lacking functional ASM exhibited a reduced viral titer after incubation with human rhinoviruses. Treatment of epithelial cells and fibroblasts with pharmacological inhibitors of the ASM revealed comparable results [25].

Here, we show that infection results in formation of glycosphingolipid-enriched membrane domains of the GM-1 (ganglioside type 1) type. Furthermore, we demonstrate the interaction of rhinoviruses and distinguishable membrane domains by *in situ* studies using rhinoviruses with fluorochrome-labeled genomic RNA. Disruption of membrane rafts by methyl-β-cyclodextrin, nystatin or filipin prevented membrane domain and platform formation and cellular infection with rhinoviruses. Moreover, we observed that GM-1 positive membrane platforms correspond at least in part to ceramide-enriched membrane platforms. We addressed the question, whether GM-1 positive membrane platforms are derivatives of ceramide-enriched platforms synthesized by the ASM. Administration of ASM specific siRNA down-regulated the formation of ceramide-enriched platforms as well as of GM-1 positive membrane platforms. This suggests that the formation of GM-1 positive membrane domains is also dependent on activation of the ASM at least for some strains of rhinoviruses. Finally, we established an experimental model using primary cells from nasal epithelial tissue to examine the rearrangement of lipids upon rhinoviral infection *ex vivo*. The results indicate that distinct membrane domains are functional in rhinoviral infections *in vivo*.

Material and Methods

Cell culture, viral stocks and labeling of rhinoviruses

Epithelial cells and fibroblasts were purchased from ATCC (HeLa epithelial cells ATCC stock number: CCL-2; Wi-38 fibroblasts ATCC stock number: CCL-75) and cultured in MEM medium (HeLa cells) supplemented with 10% FCS, 10 mM HEPES, 2 mM L-glutamine, 1 mM sodium pyruvate, 100 µM non-essential amino acids, 100 units/ml penicillin, 100 µg/ml streptomycin (all purchased from GIBCO/BRL-Life Technologies, Grand Islands, N.Y., USA).

Human rhinovirus type 2 and type 14 (RV2 and RV14) were purchased by ATCC (human rhinovirus type 2 ATCC #21112, human rhinovirus type 14 ATCC #284) and propagated by infection of HeLa cells with a multiplicity of infection (MOI) of 0.01 in DMEM medium supplemented with 2% FCS and 20 mM $MgCl_2$ referred to as infection medium to enhance viral adsorption. Adsorption of the virus was allowed for 1 hr at 37°C followed by removal of the medium and culture in standard medium for 3-4 days at 33°C. Culture at 33°C resembles the temperature condition in the nasal epithelium and leads to more efficient replication of rhinoviruses. Samples were centrifuged for 10 min at 600xg to separate cellular debris and intact cells. Viruses in the supernatant were collected and stored at -80°C.

Rhinoviruses were purified by ultracentrifugation on a sucrose gradient [26]. Purified rhinoviruses were non-covalently labeled by incubation with a RNA binding dye (Ribogreen TM Molecular Probes, Eugene, Oregon, USA) as previously described [27]. Labeled rhinoviruses were separated from non-incorporated fluorochrome by additional centrifugation in a Centricon MW 100 filter system as recommended by the manufacturer (Millipore GmbH, Schwalbach, Germany). Viral titers were measured by performing TCID Assays in triplicate. HeLa cells were seeded in 96-well plates at a density of $5x10^4$ per well, cultured up to 60-70%

confluency and infected as described above. After four days at 33°C cell layers were stained with crystal-violet (0.07% w/v in EtOH). The viral titers were determined by calculating the tissue culture infective dose (TCID 50/ml) according to the method of Blake and O'Connell [28].

Infection and treatment of cultured cells

Rafts in cultured cells were destroyed by incubation with nystatin (final concentration 10 - 30 µg/ml), filipin (final concentration 0.5 – 1.5 µg/ml) or methyl-β-cyclodextrin (final concentration: 1 mM; all obtained from Sigma) that were added to the cells 30 min prior to infection. These agents interfere with cholesterol metabolism resulting in the disruption of rafts. The inactive isomer α-cyclodextrin (final concentration 1 mM) served as control. For the formation-inhibition of ceramide-enriched membrane platforms and GM-1 positive membrane platforms respectively, cholera toxin-subunit B was added at a final concentration of 2.5 µg/ml and anti-ceramide antibody MAB15B4 at a final concentration of 2.5 µg/ml (both supplied by Sigma) 15 min before infection. For control studies cells were pretreated with a RV2 neutralizing antibody (rabbit antiserum, diluted 1:100 [29], courtesy of Prof. Dr. D. Blaas, University of Vienna, Austria) or biotin-labeled transferrin as described elsewhere [30]. Cells were washed and infected with RV2 and RV14 at an MOI of 20 in infection medium. Rhinoviruses were allowed to attach to the cells at 37°C for 10 min and cells were washed in PBS (137 mM sodium chloride, 10 mM phosphate; 2.7 mM potassium chloride, pH 7.2; phosphate-buffered saline) supplemented with $MgCl_2$ and $CaCl_2$ (5 mM each). Infection was terminated after the indicated time and cells were subjected to *in situ* staining techniques as given below. In studies that addressed effects of infection beyond 15 min, virus-containing medium was replaced by fresh complete medium and cells were maintained in complete medium for the indicated time prior to washing and fixation in 2% PFA/PBS (Paraformaldehyde in PBS).

Recovery of rhinoviruses from nasal tissue

Ex vivo nasal mucosa (Ethic comission of the University Clinics Essen-Duisburg permission number: 06-3127) were cut into pieces of 10 mg fresh weight, rinsed twice in PBS and equilibrated in MEM complete medium for 2 hrs. Cells were infected with RV2 or RV14 for 2 hrs at 37°C with 10^8 pfu/ml in infection medium. Samples were washed vigorously after infection and subjected to four freeze-thaw cycles to release virus from the cells. The samples were centrifuged at 5000xg at 4°C for 10 min to remove debris and the supernatants were collected. The supernatants were used for reinfection of HeLa cells in a modified plaque-assay. Since the number of rhinoviruses in these supernatants reflects the number of viruses that had previously infected the nasal epithelial cells, a reinfection enables the calculation of the TCID. To this end, $5x10^4$ HeLa cells were cultured in a 96-well plate up to 60-70% confluency, exposed to the supernatants obtained from the nasal tissues and death of HeLa cells served as a measurement for viral titers which was assessed after 12 and 24 hrs by TCID assay as described above.

If indicated, methyl-ß-cyclodextrin and α-cyclodextrin respectively (final concentration 5 mM), were added to the nasal tissues and were present throughout the total 4 hrs equilibration and infection period.

Immunohistochemistry

Rabbit polyclonal anti-RV2 and monoclonal anti-RV2 8F5 [29] were a courtesy of Prof. Dr. D. Blaas (University of Vienna, Austria). All other primary and secondary antibodies were purchased from Santa Cruz Biotechnologies. Biotin-labeled choleratoxin and APC-labeled Streptavidin were obtained from Sigma.

Human nasal mucosa were handled according to the protocols used for establishing primary culture cells [31, 32]. Pieces of tissues (approximately 5x5x5 mm^3 blocks) were rinsed twice with PBS supplemented with $MgCl_2$ and $CaCl_2$ (5 mM each). The samples were infected as described above with RV2 and RV14 for 2 hrs, cells were fixed in 2% PFA in PBS (pH 7.4) for 30 min at 37°C and stained with FITC-coupled cholera-toxin B-subunit (1:100 diluted) to detect ganglioside type1 (GM-1). Alternatively, GM-1 was detected by incubation with non-labeled cholera-toxin-B subunit and usage of an anti-cholera-toxin-B subunit specific antibody (anti CTX-B polyclonal antiserum, 1:200 diluted, Sigma). After staining, the tissue was washed twice, dissected mechanically and analyzed by fluorescence microscopy.

Cultured epithelial cells (HeLa cells) were grown on cover slides overnight under standardized growth conditions, infected as described above, washed twice in PBS supplemented with 5 mM each $MgCl_2$ and $CaCl_2$ and fixed in 2% PFA in PBS (pH 7.4) for 10 min. Cells were washed twice in PBS and non-specific binding sites were blocked by incubation in BSA dissolved in PBS (1% w/v) for 30 min. The anti-RV2 serum was pre-absorbed for 30 min at room temperature on non-infected HeLa cells. Subsequently, the cells were washed in PBS and incubated with pre-absorbed anti-RV2 serum (diluted 1:100) for 2 hrs at room temperature. The samples were washed again and incubated with biotin-labeled cholera-toxin subunit-B (1:100 diluted in PBS) for 20 min at room temperature. Cells were washed three times with PBS and consecutively stained with FITC- and Cy3-coupled secondary antibodies and APC-labeled streptavidin, respectively. All agent concentrations were used as recommended by the manufacturer. Cells were finally washed three times in PBS and mounted in mowiol (mixture of 2.4 g mowiol (polyvinyl ethanol, Carl Roth, Karlsuhe, Germany) and 6 g glycerin in 20 ml Tris pH 8.5, supplemented with triethylendiamin, 1,4-diazabicyclo[2.2.2]octan (DABCO, Carl Roth, Karlsuhe, Germany), 0.1 % w/v). The anti-RV2 antibody 8F5 was used as previously published [30]. The anti-ceramide antibody clone 15B4 was diluted 1:50 in PBS supplemented with 5.0 % v/v FCS.

Transient genetic silencing of the ASM by siRNA

To decrease the amount of active ASM molecules HeLa cells were treated with silencer RNAs (siRNA). Two siRNAs (sequence siRNA 1: 5'-CCA UGA AAG CAC ACC UGU CdT dT-3'; provided by Dharmacon, Illinois, USA, sequence siRNA 5'-GGU UAC AUC GCA UAG UGC CdT dT-3' provided by Ambion, Texas, USA) were pooled and transfected in a final

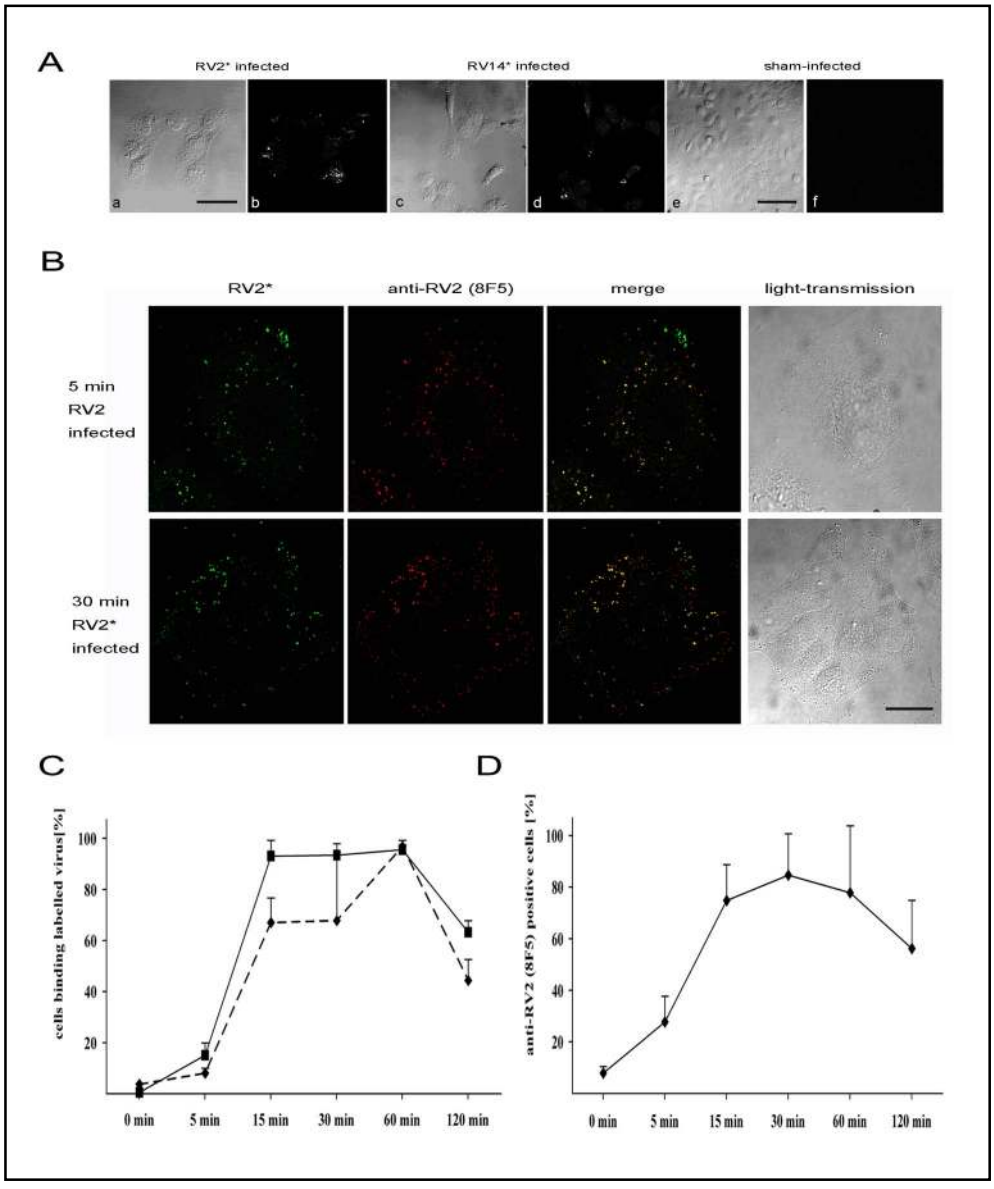

Fig. 1. Fluorochrome labeled rhinoviruses analyzed in-situ and by FACS. (A) Ribogreen labelling allows visualization of rhinoviral strains 2 (a-b, RV2*) and 14 (c-d, RV14*). Non-permeabilized HeLa epithelial cells show fluorochrome labeled rhinoviruses (b, d) clustered predominantly at the periphery (compare phase contrast images a, c) 5 min after infection. Non-permeabilized HeLa cells incubated with ribogreen-containing filtrate ("sham"-infected) showed no labelling (e-f). The figure is representative for three experiments. Scale bars in (a-b) 35 µm in (c-f) 80 µm. (B) In permeabilized HeLa cells ribogreen-labeled RV2 (RV2*) was observed in a scattered pattern from 5 to 30 min after infection. Anti-RV2 antibody 8F5 binds to the majority of ribogreen-positive particles identifying them as internalized RV2. Note that in HeLa cells clustered ribogreen-positive viruses remain 8F5 negative 5 min after infection, indicating that these viruses have not yet been internalized. All images were taken by laser scanning microscopy. The figure is representative for three experiments. Scale bar: 15 µm. (C) Time course of Hela cells infected with fluorochrome-labeled RV14 (dotted lines) and RV2 (straight lines) for indicated intervals (5, 15, 30, 60, 120 min p.i.) as analyzed by FACS. Maximal fluorescence is observed in HeLa cells 15-60 min after infection. After 60 min fluorescence decreases. Displayed is the standard deviation of three experiments. (D) Time course as determined by FACS analysis of HeLa cells infected with non-labeled RV2. Staining was performed with anti-RV2 antibody 8F5 for the indicated intervals. Displayed is the standard deviation of four experiments.

concentration of 1.25 nmol. The transfection reagent Effectin (Qiagen, Hilden, Germany) was used for siRNA shuttling according to the manufacturer's recommendations. The uptake of siRNA was determined by transfection of Alexa-488-labeled control siRNA (Qiagen, Hilden, Germany) and FACS analysis. The silencing effect of the siRNA was controlled by ASM enzyme assays as described elsewhere [33].

Microscopy and FACS analysis

Fluorescence microscopy was performed using an inverse LEICA DM IRES 2 microscope. Digitalized pictures were collected and processed using the Q-FLUORO program (Leica, Germany). Laser scanning microscopy was performed on a LEICA TSP2 module linked to a LEICA DM IRES 2 Microscope. FACS analysis of cells infected with ribogreen-labeled

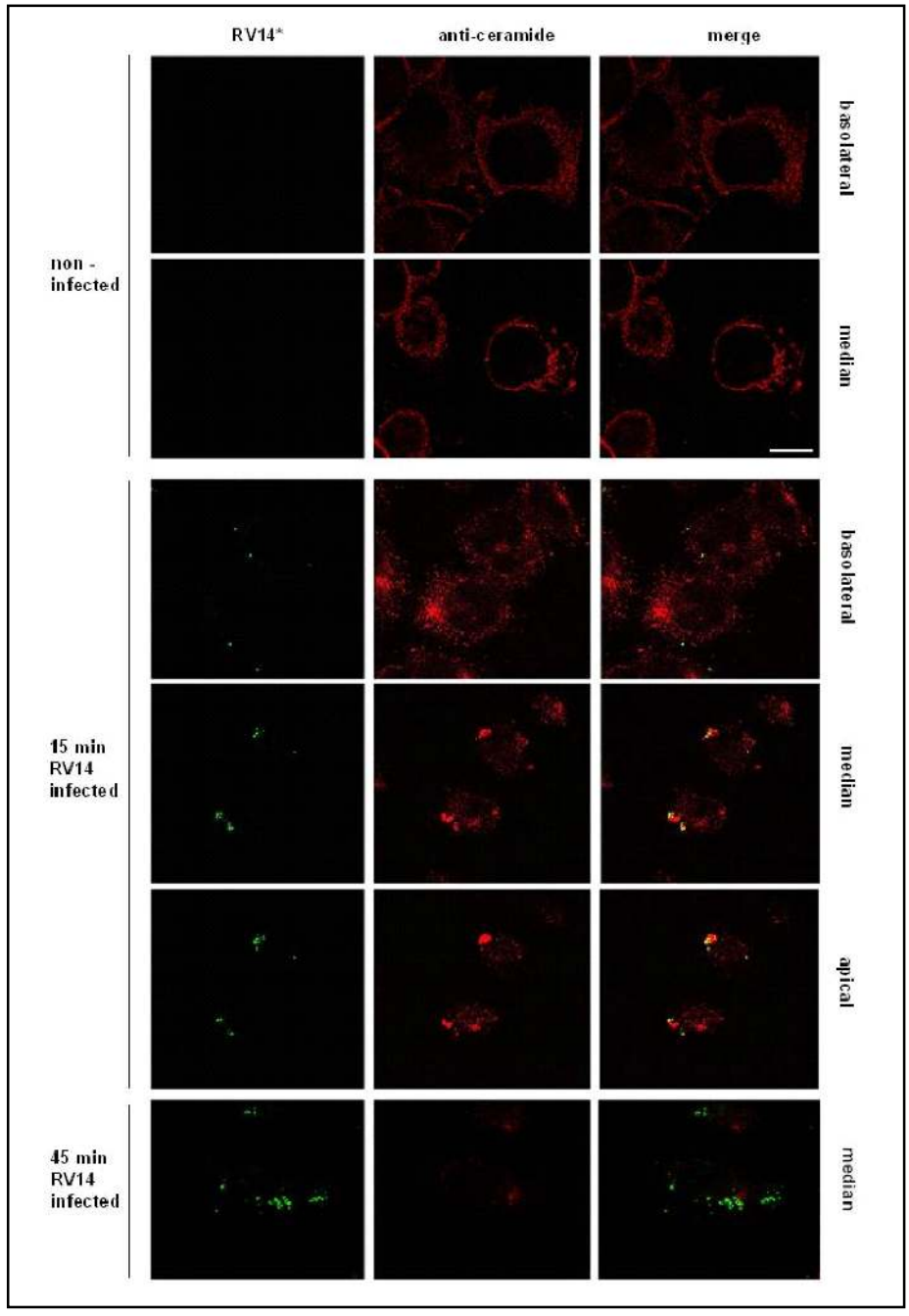

Fig. 2. Rhinoviruses interact with ceramide-enriched membrane platforms. Staining with anti-ceramide antibody showed the induction of ceramide-enriched platforms in infected HeLa cells. Merged confocal images revealed the majority of ribogreen labeled RV14 in ceramide-enriched platforms on the outer leaflet of the plasmamembrane in non-permeabilized HeLa cells. Note that co-localization of ceramide-enriched platforms was found in the median and apical optical sections rather than in basolateral sections of infected cells. In later phases of infection, i.e. 45 minutes after infection, less RV14 was found co-localized to ceramide-enriched platforms. The figure is representative for three independent experiments. Scale bar: 30µm.

rhinovirus or siRNA transfected cells was performed on a FACScalibur (BD Becton Dickinson, Heidelberg, Germany). For FACS analysis with cells infected by ribogreen-labeled rhinovirus, cells were washed in PBS after infection, fixed in Paraformaldehyde/PBS, washed again in PBS as described before. HeLa cells which were infected with RV2 were washed with PBS after infection, trypsinized and permeabilized by incubation in PBS, 0.1% v/v Triton-X-100 for 5 min and subsequently stained with anti-RV2 antibody 8F5 as described previously [30].

Results

Fluorochrome-labeling of the rhinoviral genome enables tracking of virus in vitro

In a first experiment we infected HeLa cells with purified, fluorochrome-labeled rhinoviruses of the strains 2 (minor group) or 14 (major group). Control experiments employing the ribogreen-containing filtrate resulting from the purification procedure excluded a significant

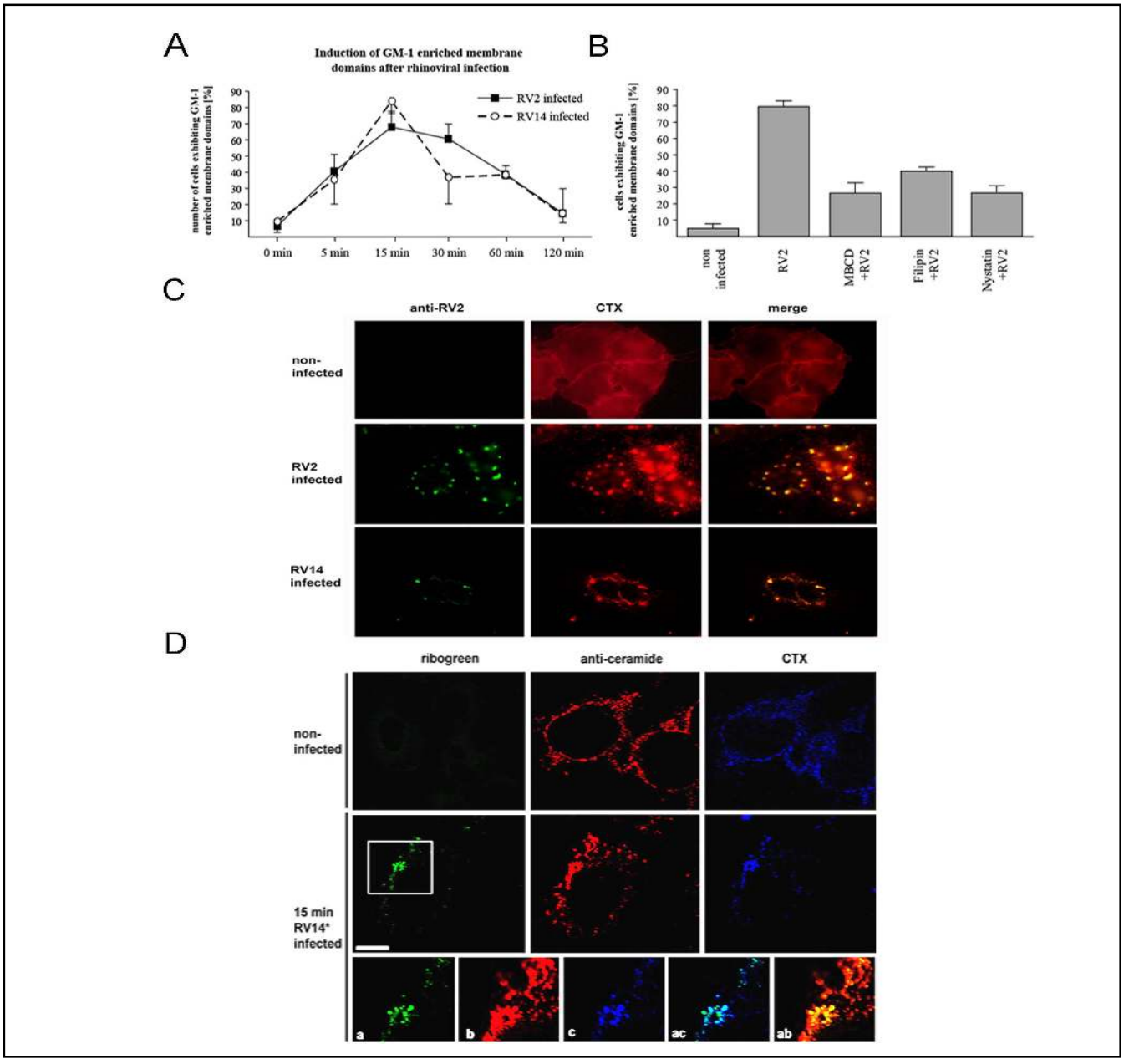

Fig. 3. Rhinoviruses induce GM-1 and co-localize to GM-1 and ceramide-enriched membrane platforms. (A) Upper panel: Induction of GM-1 positive membrane platforms during early phases of infection. Time-course of a FITC-cholera-toxin-B staining of RV2 and RV14 infected HeLa cells. Data are representing four independent experiments, which each included the analysis of 1000 cells/time point. Displayed is the mean standard deviation. Lower panel: Cholesterol-depleting drugs interfere with the formation of GM-1 positive membrane platforms in RV2 infected cells 15 minutes after infection. Note that we obtained similar results for RV14 infected cells. Data are representing five independent experiments, which each included the analysis of 1000 cells/inhibitor. Displayed is the mean standard deviation. (B) Cholera-toxin subunit-B (CTX-B) positive membrane domains are formed at the plasmamembrane and co-localize with rhinovirus RV2. The epithelial cell line HeLa was left uninfected (upper panel) infected with RV2 for 10 min (central panel), stained as indicated with CTX-B and the anti-RV2 antisera (rabbit polyclonal), and analyzed by fluorescence microscopy. Confocal image analysis of a median section of RV14 infected cells (lower panel). The figure is representative for four experiments. (C) Triple-staining of non-infected or RV14 infected cells. HeLa cells were stained with anti-ceramide, cholera-toxin-B and visualized with anti-IgM-Cy3 or anti-CTX-B-Cy5 antibody 15 minutes after infection. In infected cells, ribogreen labeled-RV14 interacts with ceramide and cholera-toxin-B-positive membrane domains. Confocal imaging of non-permeabilized cells, smaller windows show a higher magnification of the indicated area (a ribogreen, b anti-ceramide, c Cy5-cholera-toxin-B, ab overlay of a and b, ac overlay of a and c). The figure is representative for three experiments. Scale bar: 20μm.

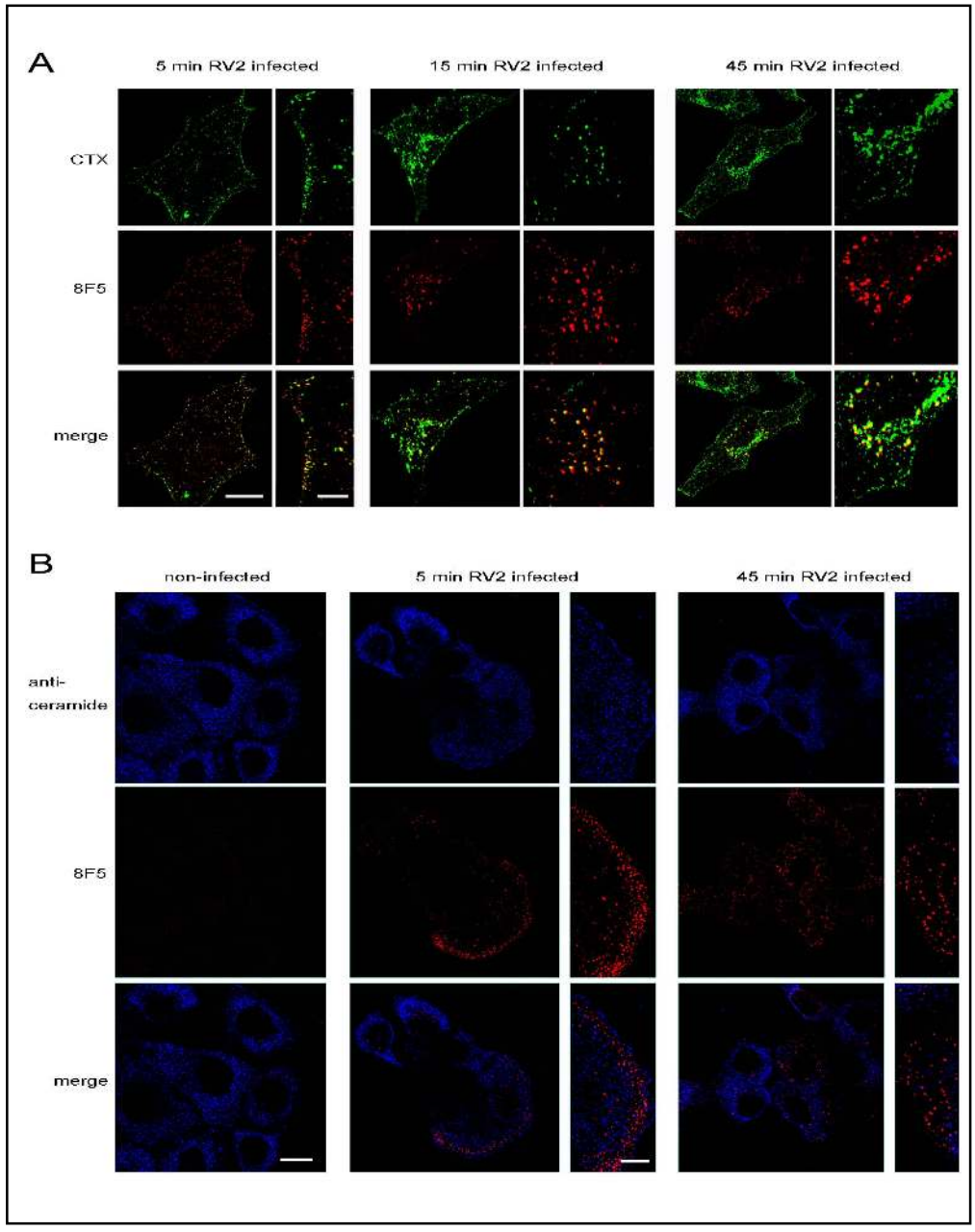

Fig. 4. GM-1 positive membrane platforms and rhinovirus interact in intracellular compartements. (A) Double immunostaining with FITC-cholera-toxin-B and anti-RV2 antibody 8F5 in a time-course experiment. Shown are confocal imaging sections of fixed and permeabilized Wi-38 fibroblasts infected for 5, 20 and 45 min intervals. Anti-RV2 antibody binding was detected by a Cy-3 coupled secondary anti-mouse antibody. Scale bar: 15 µm in panels displaying whole cells and 4 µm in panels displaying higher magnifications of subcellular areas. (B) Double immunostaining with anti-ceramide antibodies (detected by Cy3-coupled secondary antibodies) and anti-RV2 antibodies 8F5 (Cy5-coupled secondary antibody) in RV2 infected cells. Viral particles are scattered intracellularly and ceramide was not found co-localized significantly to internalized rhinoviruses. Smaller frames represent higher magnifications of sections out of the pictures to their left. The figure is representative for three independent experiments. Scale bar: 15 µm in panels displaying whole cells and 4 µm in panels displaying higher magnifications of subcellular areas.

background staining with this novel procedure. Infected HeLa cells exhibited an intense staining, characterized by single or clustered particles representing most likely viral capsids (Fig. 1A). To clarify this finding, we incubated HeLa cells infected by ribogreen-labeled RV2 with the anti-RV2 antibody 8F5, which predominatly detects internalized rhinoviruses. The ribogreen positive particles were co-stained by the anti-RV2 antibody, confirming the specificity of the labelling procedure and the integrity and viability of the virus (Fig. 1B). We observed clusters of ribogreen-labeled, 8F5-negative capsids at the cell membrane, representing attached but yet not incorporated rhinoviruses (Fig. 1B).

Next, we assessed the binding and uptake of ribogreen-labeled rhinoviruses by FACS analysis. The number of HeLa cells loaded with ribogreen-positive rhinoviruses increased from 5 to 15 minutes after infection. After 60 minutes of infection the number of HeLa cells infected with ribogreen-labeled viruses decreased. A comparison of the data with FACS studies of RV2 infected HeLa cells stained with the anti-RV2 antibody 8F5 revealed very similar results, again

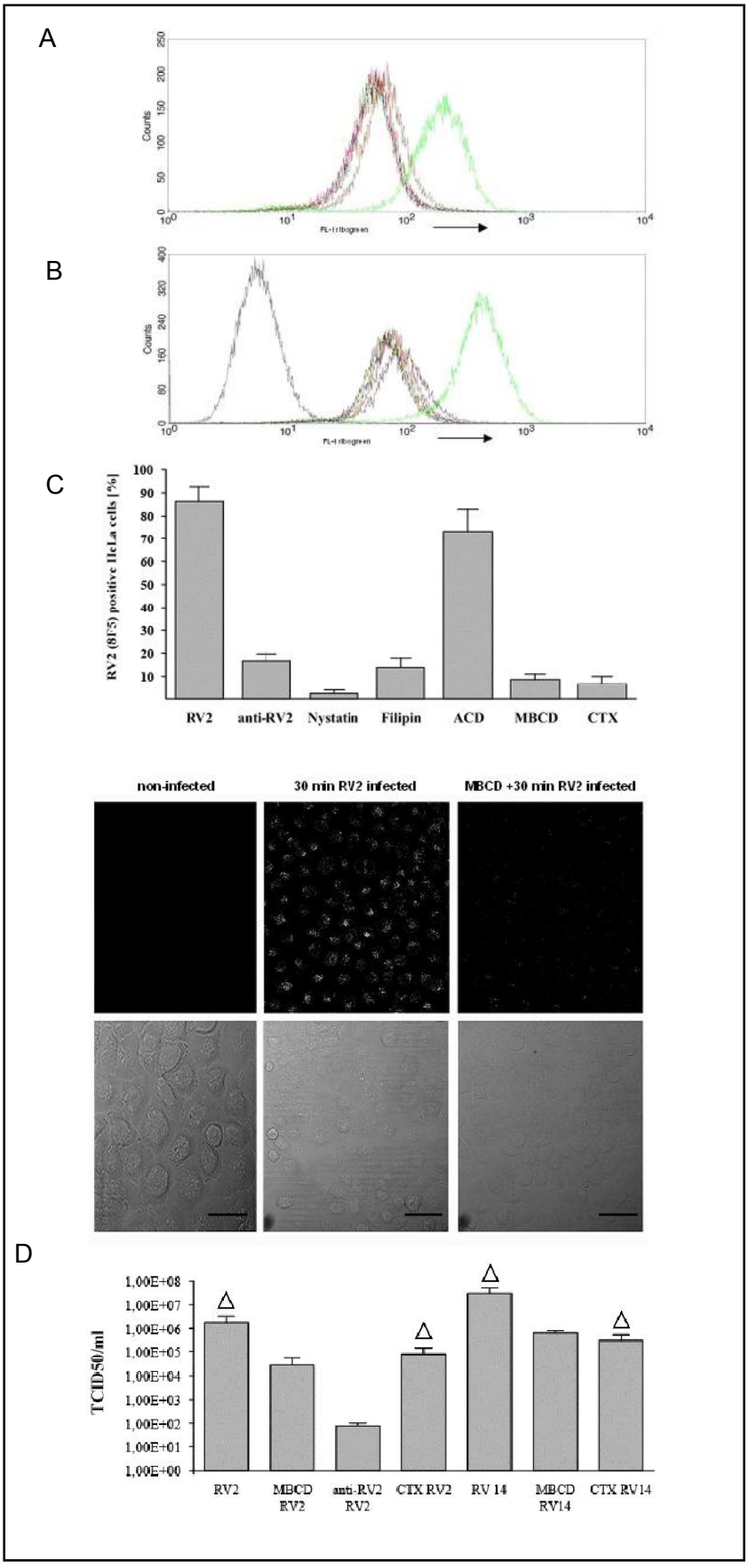

Fig. 5. Depletion of cholesterol and treatment with membrane domain neutralizing agents interfere with rhinovirus internalization and propagation. Ribogreen labeled RV2 (A) and RV14 (B) were used in a FACS analysis. The histograms present fluorescence emission of HeLa cells in the non-infected state (grey line) or infected with RV2 and RV14 (green lines in A and B) for 30 min. HeLa cells were pretreated with methyl-ß-cyclodextrin (MBCD, red lines), nystatin (brown lines), filipin (yellow lines), cholera-toxin-B (blue lines) and monoclonal anti-ceramide antibodies (black lines). In the reciprocal experiment HeLa cells were infected with RV2 and submitted to anti-RV2 8F5 staining in absence or presence of methyl-β-cyclodextrin (MBCD) as indicated. The figure is representative for three independent experiments which include the analysis of 100.000 cells. (C) Similar experiment as shown in (A) and (B) employing non-labeled RV2. RV2 internalization was assessed by staining with anti-RV2 antibody 8F5. The interference of cholesterol-depleting agents and CTX-B with RV2 internalization is given in the chart. Confocal imaging of 8F5 staining in non-infected (left) RV2-infected (central) and methyl-β-cyclodextrin-pretreated and RV2-infected (right) HeLa cells are given below the chart. Scale bar: 50 µm in panels displaying non-infected cells and 20 µm in panels displaying RV2-infected / methyl-β-cyclodextrin-pretreated and RV2-infected HeLa cells. The data represent the results of five independent experiments and include the analysis of 1000 cells/inhibitor. (D) Summary of TCID assays, demonstrating the reduction of viral titers after depletion of cholesterol and pretreatment with cholera-toxin B-subunit (CTX-B). Quantification of viral titers by TCID50 assays of cells infected with RV2 and RV14. Preincubation with methyl-β-cyclodextrin (MBCD) as well as cholera-toxin B-subunit (CTX-B) reduces the viral titer after infection. Preincubation with rhinovirus-neutralizing antibodies served as control for the inhibitory effect. Displayed is the mean standard deviation of six experiments. Open triangles represent the results of a Student‘s T-test ($P<0.05$).

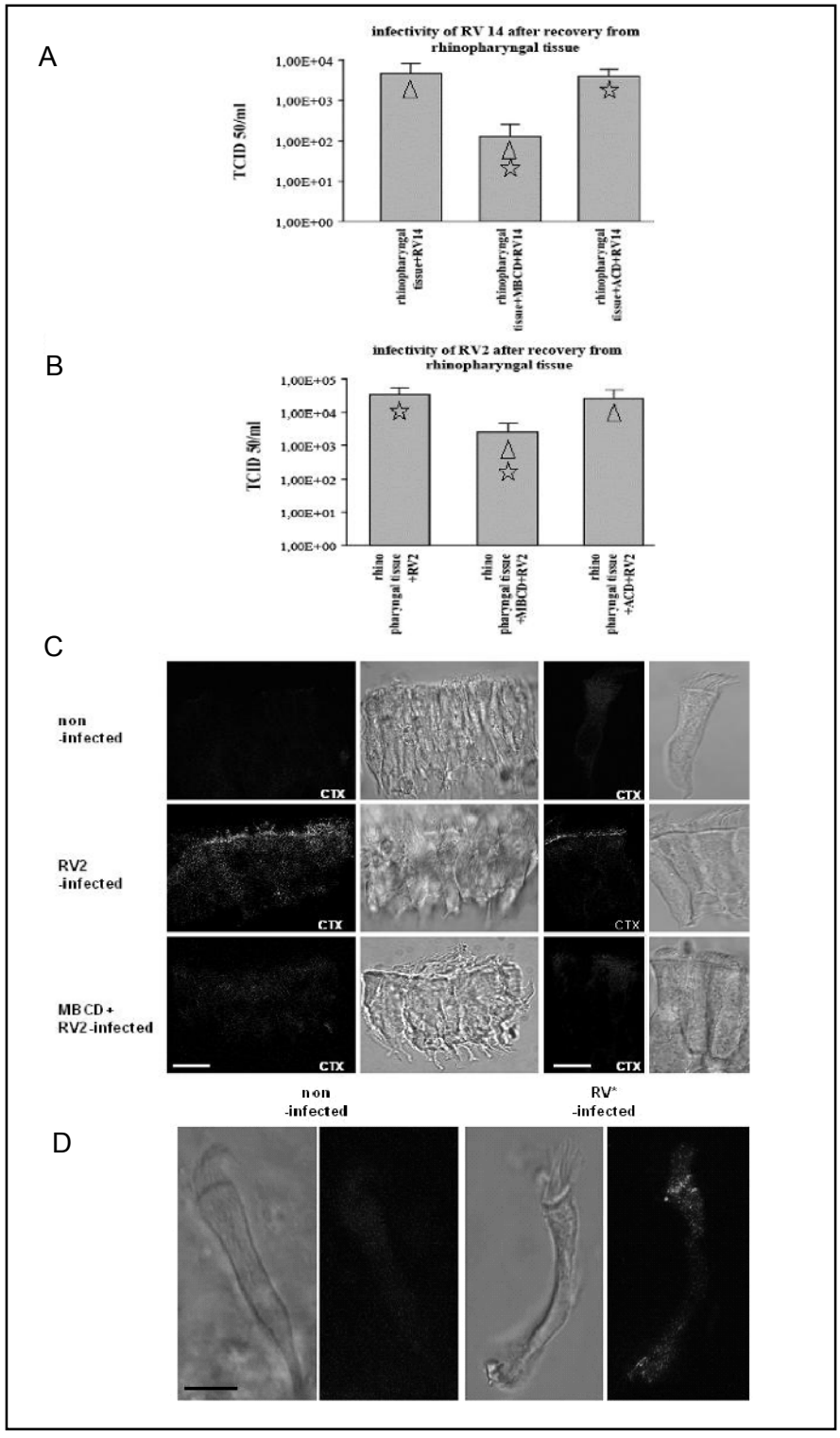

Fig. 6. Infection of human epithelial cells with rhinovirus triggers membrane platforms that are required for viral uptake. (A-B) Nasal mucosa were infected with human RV2 and RV14, washed extensively, harvested and the lysates were used to re-infect HeLa epithelial cells. Infectivity of rhinoviruses harvested from epithelial cells was determined by TCID assays. The charts display the mean standard deviation of four independent experiments. Triangles and stars, respectively, represent the results of Student's T-tests (triangles: $P< 0.05$; stars: $P< 0.1$). (C) Nasal epithelial cells were prepared from fresh nasal mucosa, infected with RV2 or left untreated, fixed and stained with FITC-labeled cholera-toxin subunit-B. Confocal image sections show GM-1 positive membrane platforms at the apical surface of ciliated epithelial cells upon infection. Pretreatment of epithelial cells with 5 mM methyl-β-cyclodextrin (MBCD) prevents the formation of membrane platforms by rhinoviral infection. The panels display the fluorescence staining and light microscopy analysis. The figure is representative for three experiments. Scale bar: 20µm. (D) Nasal epithelial cells as in (C), left untreated or infected with ribogreen-labeled RV. Confocal image sections show ribogreen-labeled viral particles predominantly at the apical, ciliated portion of cells. The figure is representative for one infection with RV14 and two experiments employing RV2. Scale bar: 15µm.

suggesting that the measurement of ribogreen positive HeLa cells identifies internalization of rhinoviruses (Figs. 1 C and D). The results showed that this novel procedure enables tracking of rhinoviruses in proceeding infections *in vitro*.

Rhinovirus strains 2 and 14 co-localize to ceramide- and GM1-enriched membrane platforms

Next, we wanted to determine the topology of rhinoviral infections, i.e. if rhinoviruses bind to distinct

sites of the plasma membrane. HeLa epithelial cells were infected with ribogreen-labeled RV14 and RV2, respectively, for 5 min to 45 min and stained with monoclonal anti-ceramide antibodies without permeabilization. In the non-infected cells ceramide was equally distributed in the outer leaflet of the plasma membrane. Upon infection with rhinovirus, the amount of ceramide increased and ceramide aggregated in platforms (Fig. 2). Confocal imaging showed a co-localization of RV14 and RV2 with ceramide-enriched membrane platforms within the early phase of the infection, i.e. within 5 - 15 minutes after infection (Fig. 2). Almost 80% of infected cells exhibited a co-localization of viral particles with ceramide-enriched platforms localizing in median and apical sections, whereas only few viral particles co-localized to ceramide-enriched platforms in basolateral sections. In samples infected for 45 min the number of cells exhibiting a localization of rhinoviruses within ceramide-enriched membrane platforms decreased to 45% and more rhinoviruses localized to regions without ceramide-enriched membrane platforms (Fig. 2). To further analyze the potential of human rhinoviruses to induce or recruit membrane domains distinct from ceramide-enriched platforms, we tested non-infected and rhinoviral infected HeLa cells for their CTX-B (cholera-toxin-B) binding. CTX-B binds to GM-1 (ganglioside type 1), a sphingolipid present in many membrane domains. Indeed, the infection with rhinoviruses induced GM-1 positive membrane platforms resembling the induction of ceramide-enriched platforms regarding the temporal course and intensity (Fig. 3A) [25]. Pretreatment of HeLa cells with cholesterol depleting drugs reduced the formation of GM-1 positive membrane platforms significantly 15 minutes after infection (Fig. 3A). *In situ*, GM-1 positive membrane platforms also exhibit the capacity to interact with rhinoviruses (Fig. 3B) from 5 to 30 minutes after infection. Therefore, we performed a double immunostaining using anti-ceramide antibodies, anti-cholera-toxin-B antibodies and compared the spatial distribution of GM-1 lipids and ceramide before and after infection with ribogreen-labeled rhinoviruses (Fig. 3C). The anti-ceramide and the cholera-toxin-B staining resulted in a homogenous fluorescence in non-infected HeLa cells. In infected cells, ribogreen-positive viral capsids clustered in membrane regions positive for both ceramide and GM-1 (Fig. 3C), suggesting a dynamic remodeling of membrane domains encountered by human rhinoviruses. The results indicated that both rhinoviral strains co-localize to cholera-toxin-B positive, GM-1 positive membrane platforms (Fig. 3B).

GM-1 positive membrane platforms also associate with intracellular viruses

Next, we investigated the role of sphingolipid-enriched membrane platforms in the intracellular traffic of rhinoviruses. To this end, we stained permeabilized and infected HeLa cells for GM-1, ceramide and rhinovirus. While we detected rhinoviruses associated with intracellular GM-1-enriched vesicular structures within HeLa cells (Fig. 4A), we were unable to detect rhinovirus associated with intracellular ceramide-enriched platforms (Fig. 4B). GM-1 positive vesicles co-localizing with rhinoviruses were predominantly grouped beyond the plasma membrane (Fig. 4A, left panel) 5 min after infection, while at 15 min after infection, RV2 loaded, GM-1 positive vesicular structures localized to perinuclear regions (Fig. 4A, central panel). Finally, 45min after infection GM-1 enriched vesicles were shuttled back to the plasma-membrane, while RV2 positive vesicles remained in the perinuclear region of the cells (Fig. 4A, right panel). Comparable results were obtained for RV14 (data not shown). The latter results suggest that rhinoviruses are transported from the plasma membrane to an intracellular compartment in vesicles enriched with GM-1.

Destabilization and neutralization of membrane domains interferes with the uptake and reproduction of rhinoviruses

Recent studies suggested interactions of rhinoviruses and ceramide-enriched platforms [25, 34]. This prompted the question whether drugs that destabilize or neutralize membrane domains affect the attachment and/or uptake of rhinoviruses. The results reveal that pretreatment with cholesterol depleting drugs reduced the attachment and/or uptake of ribogreen-labeled RV2 and RV14 at least 10-fold. The inactive stereoisomer α-cyclodextrin was without effect (Figs. 5A and B). To further confirm the role of ceramide-enriched membrane platforms for rhinoviral attachment and/or uptake we applied anti-ceramide antibodies in order to compete with the interaction of rhinoviruses with these platforms. Additionaly, we selected the compound CTX-B, which binds the biochemically related sphingolipid GM-1 to clarify the role of other sphingolipids in respect to its rhinoviral binding capacity. The results demonstrate that addition of anti-ceramide antibodies and CTX-B, repectively, significantly inhibited rhinoviral attachment and/or uptake (Figs. 5A and B). To rule out that CTX-B blocks any internalization process non-specifically, we tested the transferrin uptake in cells treated with CTX-B

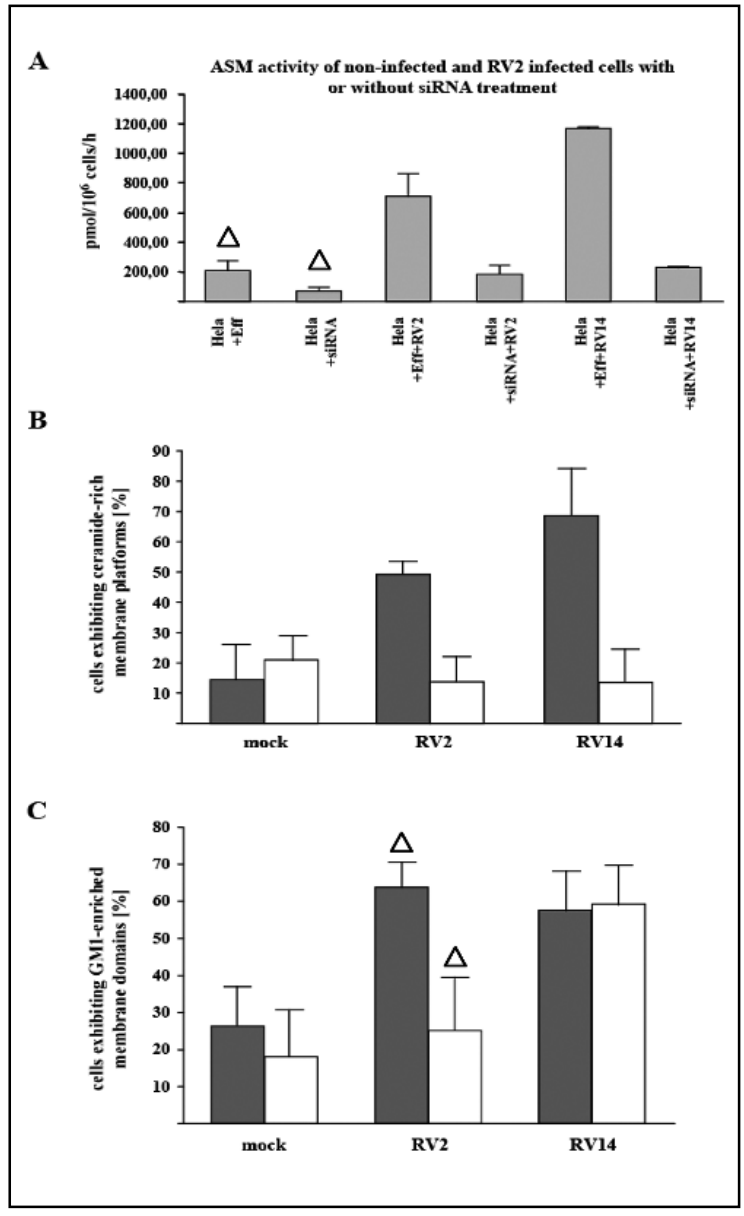

Fig. 7. Induction of the acid sphingomyelinase causes the formation of GM-1 positive membrane platforms in RV2 infected cells. (A) HeLa epithelial cells were subjected to siRNA transfection, silencing the acid sphingomyelinase (ASM). Two days after transfection the ASM activity of cells was assessed by an enzymatic assay. The ASM activity prior and after infection with RV2 and RV14 was compared in siRNA transfected and non-transfected cells. Activity of the ASM was displayed by the enzymatic degradation of radiaoactive sphingomyelin [33]. (B) Shown is the effect of ASM-downregulation by siRNA on the formation of ceramide-enriched membrane platform formation. Grey columns give the number of ceramide-enriched membrane platforms in control-transfected cells, the empty columns in ASM-siRNA-transfected cells. Quantitative analysis of non-infected, RV2 and RV14 infected HeLa epithelial cells. (C) Effect of ASM silencing by siRNA treatment (grey columns: control-transfected, open columns: siRNA-transfected cells) on the formation of GM-1 positive membrane platforms. Quantitative analysis of non-infected, RV2 and RV14 infected HeLa epithelial cells. Data were collected from four independent experiments presenting the mean standard deviation. Open triangles represent the results of Student's T-test ($P<0.05$).

under the same conditions. We found that CTX-B did not interfere with the transferrin uptake (data not shown).

In a similar experiment we treated HeLa cells with cholesterol-depleting drugs and CTX-B, respectively, prior to infection with RV2. Again, the disruption or neutralization of rafts substantially reduced the number of cells showing internalized RV2, detected by the anti-RV2 antibody 8F5 (Fig. 5C). Next, we addressed the question whether inactivation of membrane platforms also interferes with the synthesis and release of rhinoviruses. The results reveal that methyl-ß-cyclodextrin, nystatin, filipin, CTX-B and neutralizing anti-RV2 antibody that were added 30 min prior to infection reduced viral titers by up to 100-fold in a TCID assay (Fig. 5D). In contrast, the administration of the same CTX-B concentration post-infection did not decrease the viral titer (data not shown), suggesting that the induction of GM-1 positive membrane platforms is a prerequisite for the internalization and propagation of rhinoviruses.

Induction of GM-1 positive membrane platforms in vivo

These studies demonstrated a role of sphingolipid-enriched membrane domains for the uptake as well as reproduction of human rhinoviruses. To transfer the results of our *in situ* studies to an *ex-vivo* model, we infected

small nasal polyps with intact epithelium cell layers with rhinoviruses. The depletion of cholesterol by methyl-β-cyclodextrin abolished the formation of GM-1 positive membrane platforms and impaired the infection with rhinovirus *in vivo*, while the inactive isomer α-cyclodextrin was without effect (Figs. 6A-B). Furthermore, *in situ* experiments demonstrate an increase of CTX-B at the apical surface of nasal epithelial cells 30 minutes after infection, while the surface levels of GM-1 did not change in non-infected cells. As shown for cultured cells, methyl-β-cyclodextrin diminished the induction of GM-1 positive membrane platforms in the apical surface of nasal epithelial cells (Fig. 6C). Ribogreen-labeled RV2 and RV14 were found predominantly at the apical, ciliated portion of cells (Fig. 6D). These *ex vivo* data underline the importance of GM-1 positive membrane platforms for the infection of nasal epithelial cells with human rhinovirus.

Formation of ceramide-enriched platforms and GM-1 positive membrane platforms – the role of the acid sphingomyelinase (ASM)

To address the question whether GM-1 positive membrane platforms are formed from ceramide-enriched membranes or wether GM-1 positive membrane platforms are independently generated, we suppressed expression of ASM by siRNA transfection (Fig. 7A). Control experiments confirmed that siRNA down regulated the activity of the ASM in infected and non-infected cells by 75 - 80%, while non-specific siRNA was without effect. Suppression of ASM prevented the induction of ceramide-enriched membrane platforms after infection with RV2 and RV14 (Fig. 7B). Suppression of ASM also inhibited the formation of GM-1-positive membrane platforms after transfection of HeLa cells with RV2 (Fig. 7B, C), while there was no change in the formation of GM-1 positive membrane platforms after infection with RV14 (Fig. 7C). This indicates that RV14 induces GM-1 positive membrane platforms in an ASM-independent manner, whereas RV2 infections recruit GM-1 positive membrane platforms via activation of the ASM.

Discussion

The present manuscript addressed the question if distinct membrane platforms serve as viral binding sites and are functional in the uptake and intracellular transport of rhinoviruses. We used a novel efficient labeling technique, which is advantageous because "ribogreen" enters capsids by diffusion and binds RNA non-covalently [27]. This avoids covalent linkages of dyes to capsid proteins that may interfere with the binding to receptor molecules. We controlled the quality of this labeling technique by double staining using the anti-RV2 antibody 8F5, which proved the specificity and efficiancy of labelling. In our study, the attachment of ribogreen-labeled rhinoviruses to cells was shown to be responsive to drugs, which destabilize rafts either by depleting cholesterol (methyl-β-cyclodextrin) or by sequestering intracellular cholesterol (nystatin, filipin). Previous studies provided evidence for the generation of ceramide-enriched membrane platforms by the activation of the ASM and their requirement for rhinoviral infection [25]. To further clarify, whether rhinoviruses attach to ceramide-enriched platforms, we administered anti-ceramide antibodies, which were able to compete with rhinoviruses for binding. Furthermore, our extended *in situ* studies visualized ribogreen-labeled rhinoviruses interacting with ceramide-enriched membrane platforms. Our results are in line with recent studies suggesting that interactions between rafts or ceramide-enriched membrane platforms respectively, and rhinoviruses are essential for signal transduction cascades employing phosphatidyl-inositol kinase [26, 34, 35], small GTPases and the MAP kinase P38-K [36]. A novel finding of this manuscript is the identification of GM-1 as an additional compound present in membrane domains interacting with rhinoviruses. The appearance of GM-1 in membrane domains seems to be essential not only for the attachment of rhinoviruses, but possibly for internalization of rhinoviruses by a novel yet to be characterized pathway. *In situ* we tracked ribogreen- and 8F5-labeled rhinoviruses and tested if intracellular compounds are positive for ceramide and/or GM-1. We found internalized rhinoviruses only co-localized to intracellular GM-1 enriched membrane domains, which are integrative compounds of transport vesicles. It might be possible that GM-1 positive vesicles are shuttling rhinoviruses to the endosomal compartment, which is necessary for the uncoating process [37, 38]. The results of the TCID assay underline that GM-1 enriched membrane platforms play a critical role in rhinoviral propagation. A recent study showed that RV2 engages the clathrin dependent internalization pathway, which is also sensitive to cholesterol depletion [30]. The same study excluded any direct interaction of RV2 and caveolae and suggests that RV2 viruses do not employ caveolae for entry. The utilization of novel, non-clathrin, non-caveolin dependent endocytosis pathways was recently demonstrated for SV40 [16], Influenza virus [39] and

Coxsackieviruses [40].

Most studies concentrate their experiments on cultured cells and the results do not necessarily resemble the *in vivo* situation. In this regard, the role of ICAM-1 (intercellular adhesion molecule type 1) and (V)LDLR ((very) low density lipoprotein), identified as rhinoviral receptors in cultured cells, respectively, needs further clarification. Many publications found ICAM-1 only poorly distributed on the apical surface of epithelial tissues and (V)LDL receptors are present at the basolateral and lateral surface of cells. Some publications report the up-regulation of both receptor types after rhinoviral infections [24, 41], suggesting that rhinoviruses infect nasal epithelial tissues primary via another pathway possibly engaging other receptor molecules than (V)LDL receptors and ICAM-1. For cultured cells, we demonstrate the direct interaction of viral particles and ceramide/GM1 enriched membrane platforms, which are functional in the attachment and/or internalization of rhinoviruses. GM-1 positive membrane platforms are also induced in isolated nasal epithelial cells so that our experiments suggest that GM-1 positive membrane platforms play a role in attachment and/or entry *in-vivo*.

We were also interested in the origin of GM-1 in those membrane domains to which rhinoviruses attach. As pointed out before, infection activates the ASM and causes the formation of ceramide-enriched platforms [25]. We showed here an interaction of rhinoviruses to membrane domains containing both, ceramide and GM-1, respectively. The question arise, whether GM-1 positive membrane platforms are formed independently from ceramide-enriched platforms and both entities fuse to one functional domain or whether ceramide-enriched platforms are restructured upon contact to rhinoviruses. Ceramide can be processed enzymatically to gangliosides of the GM-1 type [42]. If so, inhibition of the ASM should suppress the formation of both, ceramide-enriched platforms and GM-1 positive membrane platforms. Supression of ASM in epithelial cells by siRNA treatment indeed substantially reduced the formation of ceramide-enriched platforms upon infection. In contrast, the number of cells exhibiting GM-1 positive membrane platforms after treatment with siRNA decreased in RV2 infected cells only, whereas RV14 infected cells showed no response to the reduced concentration of ASM regarding the number of GM-1 positive membrane platforms. Thus, our results suggest a different origin of GM-1 enriched membrane domains in RV2 and RV14 infected cells.

Further studies will address the question if RV2 and RV14 activate different signal pathways leading either to the recruitment of GM-1 to ceramide-enriched membrane platforms or the generation of GM-1 on site of ceramide-enriched platforms. This dynamic process could be the committing step of a rhinoviral uptake pathway, which is further characterized by the interaction of rhinoviral particles with intracellular GM-1 positive membrane platforms.

Acknowledgements

The study was supported by grants of the IFORES program of the University of Duisburg-Essen and the Deutsche Forschungsgemeinschaft (Gu 335/10-3).

References

1 Singer SJ, Nicolson JL: The fluid mosaic model of the structure of cell membranes. Science 1972;175:720-731.

2 Simons K, Ikonen E: Functional rafts in cell membranes. Nature 1997;387:569-572.

3 Simons K, Ehehalt R: Cholesterol, lipid rafts, and disease. J Clin Invest 2002;110:597-603.

4 Brown DA London E: Functions of lipid rafts in biological membranes. Annu Rev Cell Dev Biol 1998;14:111-136.

5 Grassme H, Jendrossek V, Riehle A, von Kurthy G, Berger J, Schwarz H, Weller M, Kolesnick R, Gulbins E: Host defense against Pseudomonas aeruginosa requires ceramide-rich membrane rafts. Nat Med 2003;9:322-330.

6 Garner MJ, Hayward RD, Koronakis V: The Salmonella pathogenicity island 1 secretion system directs cellular cholesterol redistribution during mammalian cell entry and intracellular trafficking. Cell Microbiol 2002;4:153-165.

7 Kovbasnjuk O, Edidin M, Donowitz M: Role of lipid rafts in Shiga toxin 1 interaction with the apical surface of Caco-2 cells. J Cell Sci 2001;114:4025-4031.

8 Zitzer A, Bittman R, Verbicky CA, Erukulla RK, Bhakdi S, Weis S, Valeva A, Palmer M: Coupling of cholesterol and cone-shaped lipids in bilayers augments membrane permeabilization by the cholesterol-specific toxins streptolysin O and Vibrio cholerae cytolysin. J Biol Chem 2001;276:14628-14633

9 Nusrat A, von Eichel-Streiber C, Turner JR, Verkade P, Madara JL Parkos CA: Clostridium difficile toxins disrupt epithelial barrier function by altering membrane microdomain localization of tight junction proteins. Infect. Immun 2001;69:1329-1336.

10 Scheiffele P, Rietveld A, Wilk T, Simons K: Influenza viruses select ordered lipid domains during budding from the plasma membrane. J Biol Chem 1999;274:2038-2044.

11 Simpson-Holley M, Ellis D, Fisher D, Elton D, McCauley J, Digard P: A functional link between the actin cytoskeleton and lipid rafts during budding of filamentous influenza virions. Virology 2002;301:212-225.

12 Zhang J, Pekosz A, Lamb RA: Influenza virus assembly and lipid raft microdomains: a role for the cytoplasmic tails of the spike glycoproteins. J Virol 2000; 4:4634-4644.

13 Ono A, Freed EO: Plasma membrane rafts play a critical role in HIV-1 assembly and release. Proc Natl Acad Sci USA 2001;98:13925-13930.

14 Liao Z, Graham DR Hildreth JE: Lipid rafts and HIV pathogenesis: virion-associated cholesterol is required for fusion and infection of susceptible cells. AIDS Res Hum Retroviruses 2003;19:675-687.

15 Werling D, Hope JC, Chaplin P, Collins RA, Taylor G, Howard CJ: Involvement of caveolae in the uptake of respiratory syncytial virus antigen by dendritic cells. J Leukoc Biol 1999;66:50-58.

16 Pelkmans L, Kartenbeck J Helenius A: Caveolar endocytosis of simian virus 40 reveals a new two-step vesicular-transport pathway to the ER. Nat Cell Biol 2001;3:473-483.

17 Manie SN, Debreyne S, Vincent S, Gerlier D: Measles virus structural components are enriched into lipid raft microdomains: a potential cellular location for virus assembly. J Virol 2000;74:305-311.

18 Gulbins E, Dreschers S, Wilker B, Grassme H: 2004 Ceramide, membrane rafts and infections. J Mol Med 2004;82:357-363.

19 Hofer F, Gruenberger M, Kowalski H, Machat H, Huettinger M, Kuechler F Blaas D: Members of the low density lipoprotein receptor family mediate cell entry of a minor-group common cold virus. Proc Natl Acad Sci USA 1994;91:1839-1842.

20 Ronacher B, Marlovits TC, Moser R Blaas D: Expression and folding of human very-low-density lipoprotein receptor fragments: neutralization capacity toward human rhinovirus HRV2. Virology 2000;278:541-550.

21 Reithmayer M, Reischl A, Snyers L Blaas D: Species-specific receptor recognition by a minor-group human rhinovirus (HRV): HRV serotype 1A distinguishes between the murine and the human low-density lipoprotein receptor. J Virol 2002;76:6957-6965.

22 Greve J M, Davis G, Meyer AM, Forte CP, Yost SC, Marlor CW, Kamarck ME McClelland A: The major human rhinovirus receptor is ICAM-1. Cell 1989;56:839-847.

23 Matter K, Hunziker W, Mellman I: Basolateral sorting of LDL receptor in MDCK cells: the cytoplasmic domain contains two tyrosine-dependent targeting determinants. Cell 1992;71:741-753.

24 Winther B, Greve JM, Gwaltney Jr. JM, Innes DJ, Eastham JR, McClelland A, Hendley JO: Surface expression of intercellular adhesion molecule 1 on epithelial cells in the human adenoid. J Infect Dis 1997;176:523-525

25 Grassme H, Riehle A, Wilker B, Gulbins E: Rhinoviruses infect human epithelial cells via ceramide-enriched membrane platforms. J Biol Chem 2005;280:26256-26262.

26 Newcomb DC, Sajjan U, Suparna N, Yue J, Goldsmith AM, Bentley JK, Hershenson MB: PI 3-Kinase is required for rhinovirus-induced airway epithelial cell IL-8 expression. J. Biol Chem 2000;280:36952-36961.

27 Kremser L, Okun VM, Nicodemou A, Blaas D, Kenndler E: 2004. Binding of Fluorescent dye to genomic RNA inside intact human rhinovirus after viral capsid penetration investigated by capillary electrophoresis. Anal Chem 2004;76:882-887.

28 Blake K, O'Connell S: Virus culture In Harper DR (ed.), Virology labfax. Blackwell Scientific Publications, West Smithfield, London, United Kingdom 1993, pp 81-122.

29 Hewat EA Blaas D: Structure of a neutralizing antibody bound bivalently to human rhinovirus 2. EMBO J 1996;15:1515-1523

30 Snyers L, Zwickl H, Blaas D: Human rhinovirus type 2 is internalized by clathrin-mediated endocytosis. Virol 2003;77:5360-5369.

31 Jorrison M, van der Schueren B, van den Berghe H, Cassiman JJ: The preservation and regeneration of cilia on human nasal epithelial cells cultured in vivo. Arch. Otorhinolaryngol. 1989;246:308-314.

32 Ulrich M, Herbert S, Berger J, Bellon G, Louis D, Munker G, Döring G: Localization of Staphyloccocus aureus in infected airways of patients with cystis fibrosis an in a cell culture model of S. aureus adherence. Am. J. Respir. Cell Mol. Biol. 1998;19:83-91.

33 Brenner B, Grassmé HU, Müller C, Lang F, Speer CP, Gulbins E: L-selectin stimulates the neutral sphingomyelinase and induces release of ceramide. Exp Cell Res 1998;243:123-128.

34 Bentley JK, Newcomb DC, Goldsmith AM, Jia Y, Sajjan US, Hershenson MB: Rhinovirus Activates IL-8 Expression via a Src/p110{beta} PI 3-kinase/Akt Pathway in Human Airway Epithelial Cells. J Virol 2007;81(3):1186-94.

35 Kolesnik RM, Goni FM Alonso A: Compartimentalization of ceramide signaling: physical foundations and biological effects. J Cell Physiol 2000;184:285-300.

36 Dumitru CA, Dreschers S, Gulbins E: Rhinoviral infections activate p38MAP-Kinases via membrane rafts and RhoA. Cell Phys Biochem 2006;17:159-166.

37 Nurani G, Lindqvist B, Casanovas JM: Receptor priming of human rhinoviruses for uncoating and entry at mild low-pH environments. J Virol 2003;77,11985-11991.

38 Neubauer C, Frasel L, Kuechler E. Blaas D: Mechanism of entry of human rhinovirus 2 into HeLa cells. Virology 1987;158:256-258.

39 Sieczkarski SB, Whittaker GR: Characterization of the host cell entry of filamentous influenza virus. Arch Virol 2005;150:1783-1796.

40 Ashbourne Excoffon KJ, Moninger T, Zabner J: The coxsackie B virus and adenovirus receptor resides in a distinct membrane microdomain. J Virol 2003;77:(4):2559-67.

41 Suzuki T, Yamaya M, Sekizawa K, Yamada N, Nakayama K, Ishizuka S, Kamanaka M, Morimoto T, Numazaki Y, Sasaki H: Effects of dexamethasone on rhinovirus infection in cultured human tracheal epithelial cells. Am J Physiol Lung Cell Mol Physiol 2000;278:L560-L571.

42 Lovat PE, Di Sano F, Corazzari M, Fazi B, Donnorso RP, Pearson AD, Hall AG, Redfern CP, Piacentini M: Gangliosides link the acidic sphingomyelinase-mediated induction of ceramide to 12-lipoxygenase-dependent apoptosis of neuroblastoma in response to fenretinide. J Natl Cancer Inst 2004;96:1288-1299.